SUPPLEMENTARY INFORMATION

Fluidic microactuation of flexible electrodes for neural recording

Flavia Vitale[1†§], Daniel G. Vercosa[2,3†], Alexander V. Rodriguez[3], Sushma Sri Pamulapati[1], Frederik Seibt[4], Eric Lewis[3], J. Stephen Yan[5], Krishna Badhiwala[5], Mohammed Adnan[1¶], Gianni Royer-Carfagni[6], Michael Beierlein[4], Caleb Kemere[3,5,7*], Matteo Pasquali[1, 8*] and Jacob T. Robinson[2,3,5,7*]

1. Department of Chemical and Biomolecular Engineering, Rice University, Houston TX 77005
2. Applied Physics Program, Rice University, Houston TX 77005
3. Department of Electrical and Computer Engineering, Rice University, Houston TX 77005
4. McGovern Medical School at UTHealth, Department of Neurobiology and Anatomy, Houston TX 77030
5. Department of Bioengineering, Rice University, Houston TX 77005
6. Department of Engineering and Architecture, University of Parma, Parma, I-43100, Italy
7. Department of Neuroscience, Baylor College of Medicine, Houston TX 77030
8. Department of Chemistry, The Smalley-Curl Institute, Rice University, Houston, TX 77005
†These authors contributed equally to this work

*Correspondence:
Jacob T. Robinson, Department of Electrical and Computer Engineering, Rice University, Duncan Hall 2041, 6100 Main Street, MS 380 Houston, TX 77005, USA e-mail: jtrobinson@rice.edu
Matteo Pasquali, Department of Chemical and Biomolecular Engineering, Rice University, Keck Hall 229, 6100 Main Street, MS 369 Houston, TX 77005, USA e-mail: mp@rice.edu

Caleb Kemere, Department of Electrical and Computer Engineering, Rice University, BRC 727, 6100 Main Street, MS 384 Houston, TX 77005, USA e-mail: caleb.kemere@rice.edu

Current address:
[§]Center for Neuroengineering and Therapeutics, Department of Neurology, University of Pennsylvania, Philadelphia PA 19104
[¶]Abu Dhabi Financial Group, Abu Dhabi, UAE

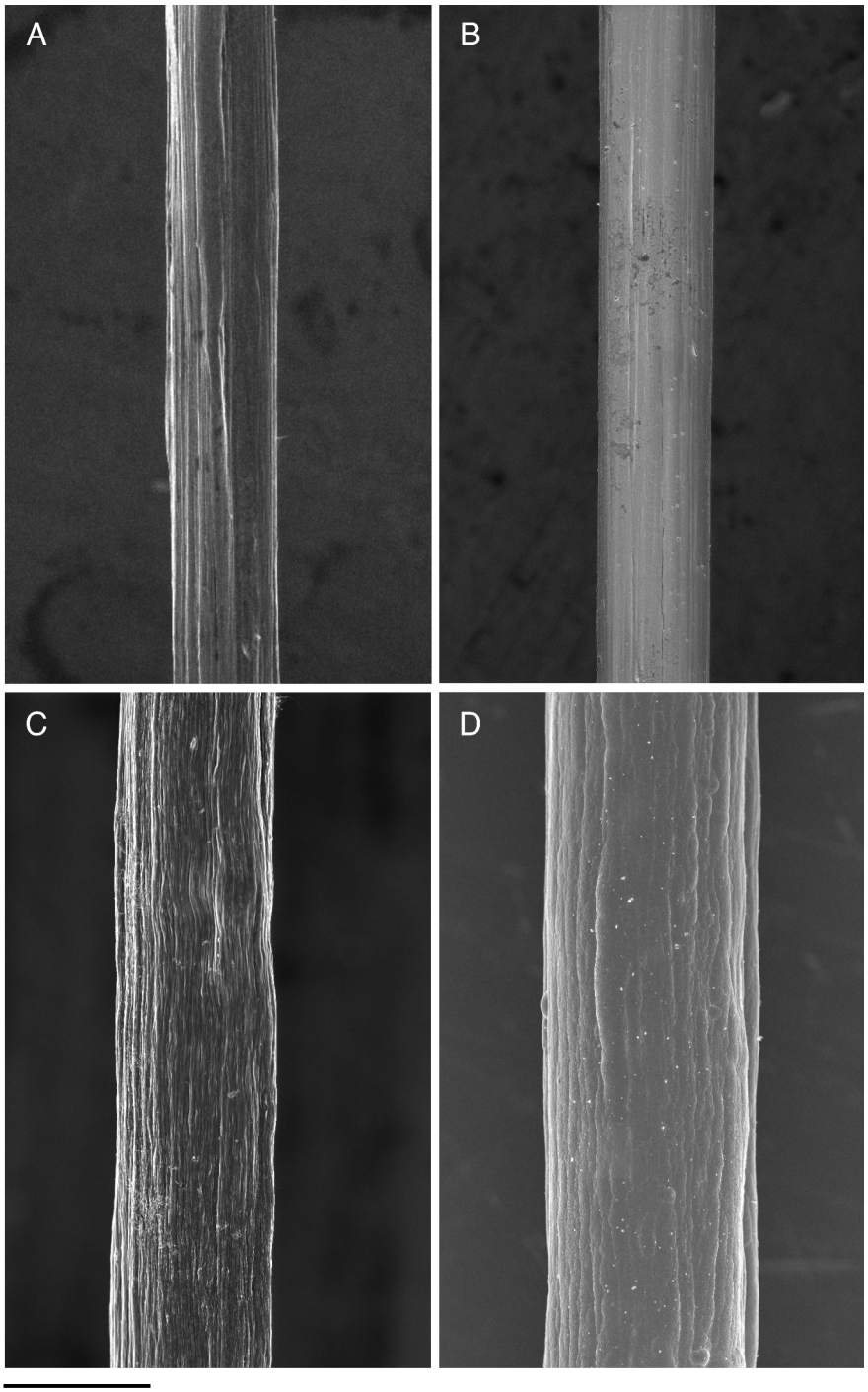

Figure S1. SEM images of CNTf: (A) as-spun (diameter 12.5 μm), (B) post Al_2O_3-HfO_2 encapsulation, (C) as-spun (diameter 23 μm) and (D) post parylene encapsulation. Scale bar: 20 μm.

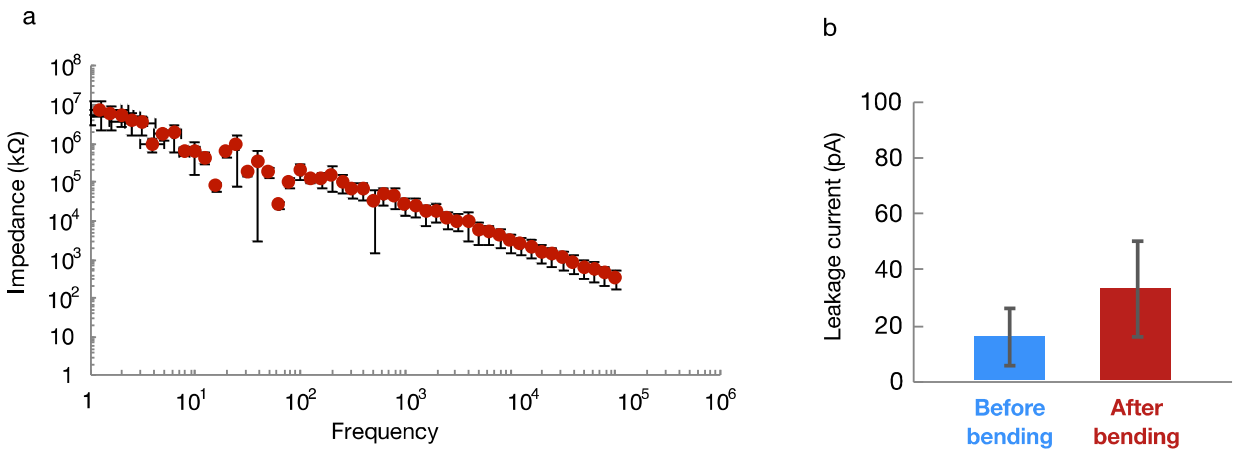

Figure S2. Characterization of the parylene insulation stability: (a) impedance spectrum of the parylene insulation on a CNTf fiber. The average modulus at 1 kHz is 25 ± 11 MΩ. (b) Leakage currents before and after bending the insulated CNTf at 90 degrees in five different points.

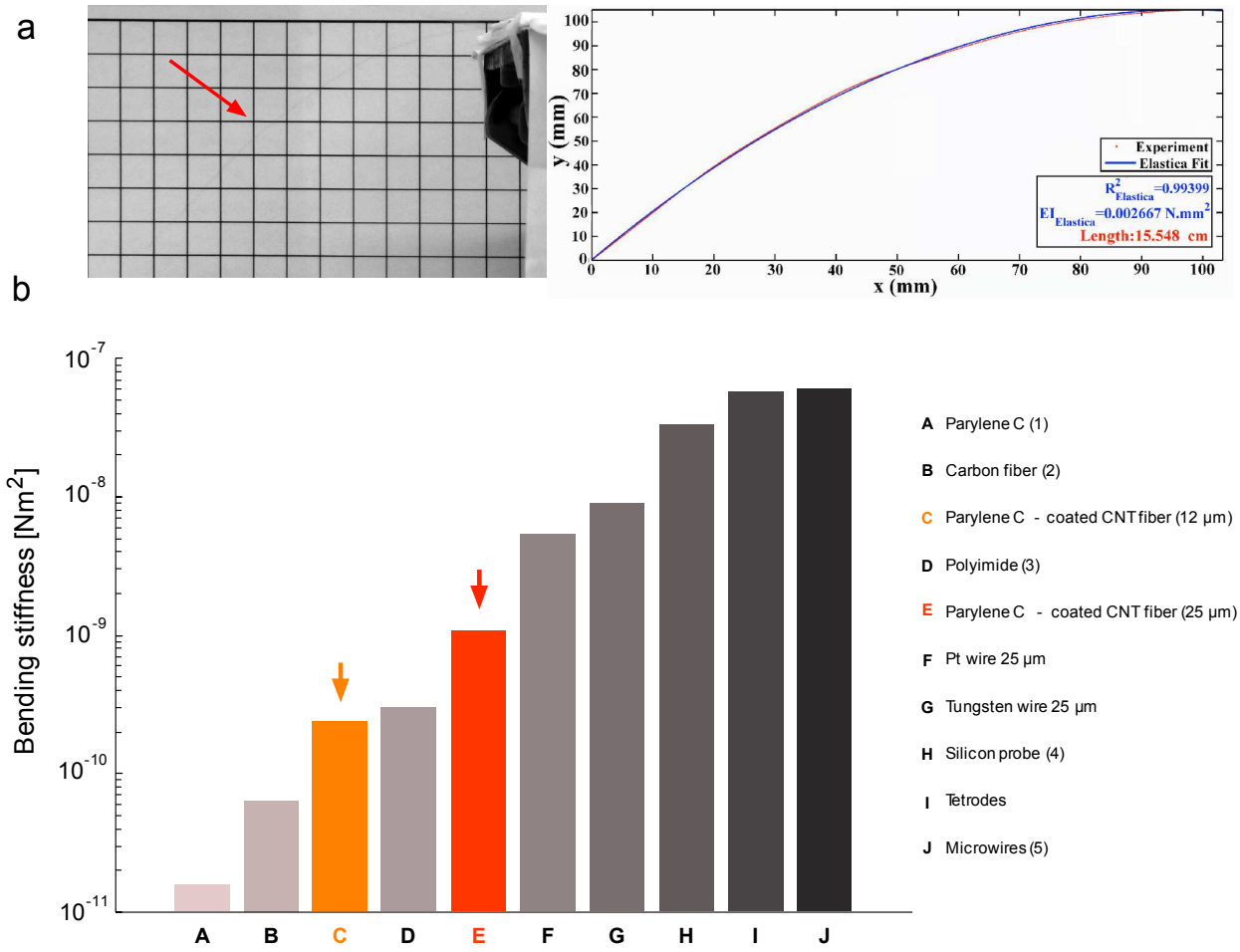

Figure S3. Bending stiffness measurements. (a) Left: representative profile of a CNTf microelectrode cantilever hanging under self-weight. Right panel shows the same profile digitally processed with Matlab and, overlaid, the fitted deformation used to calculate the bending stiffness *EI*. (b) Comparison between the bending stiffness of CNTf microelectrodes and other neural probes. The stiffness of CNTf microelectrodes with diameter of 12 µm coated with 2.5 µm thick parylene layer (orange arrow) is 0.23x10^{-9} Nm^2, comparable to that of polyimide probes, which require insertion supports. For the largest CNT fiber used in this work (25 µm, red arrow) the stiffness is 1.07 x10^{-9} Nm^2, which is 5 and 8 times lower than platinum and tungsten microelectrodes of the same diameter, respectively. The bending stiffness of CNT fibers was measured with the experimental setup described in the Methods section. The bending stiffness of probes with cylindrical cross section was calculated as: $E\pi d^4/64$, where *E* is the Young's modulus of the electrode material and *d* is the probe diameter. For shaft-shaped probes

the bending stiffness was calculated as: $Ewh^3/12$, where *w* is the width and *h* is the thickness of the shaft, similar to other calculations of bending stiffness of neural probes[6].

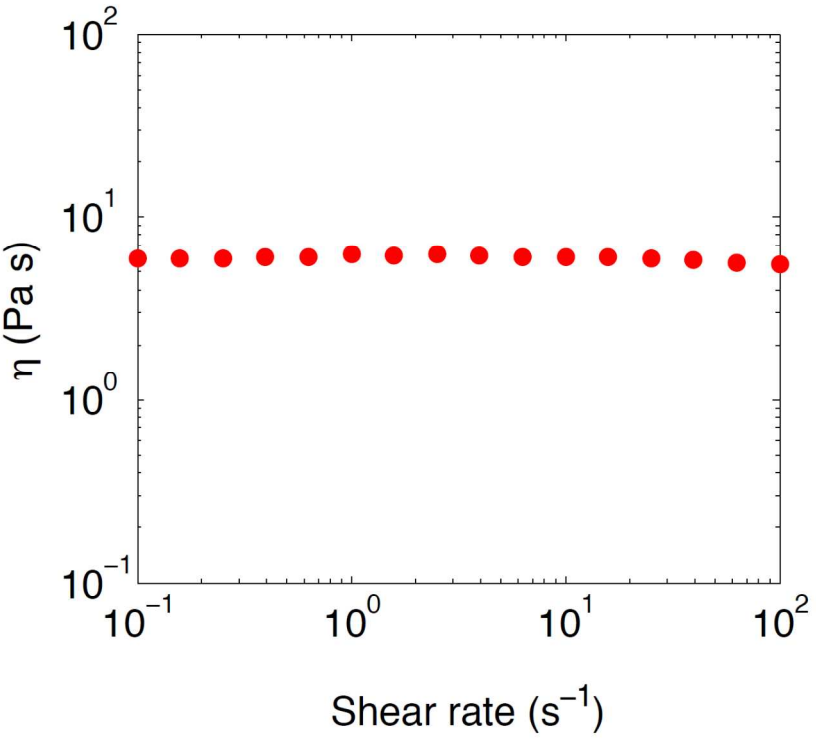

Figure S4. Shear rheometry of the 40% Dextran aqueous solution used for CNTf flow. As expected, the solution behaves as a Newtonian fluid and the viscosity is not affected by changes in the shear rate.

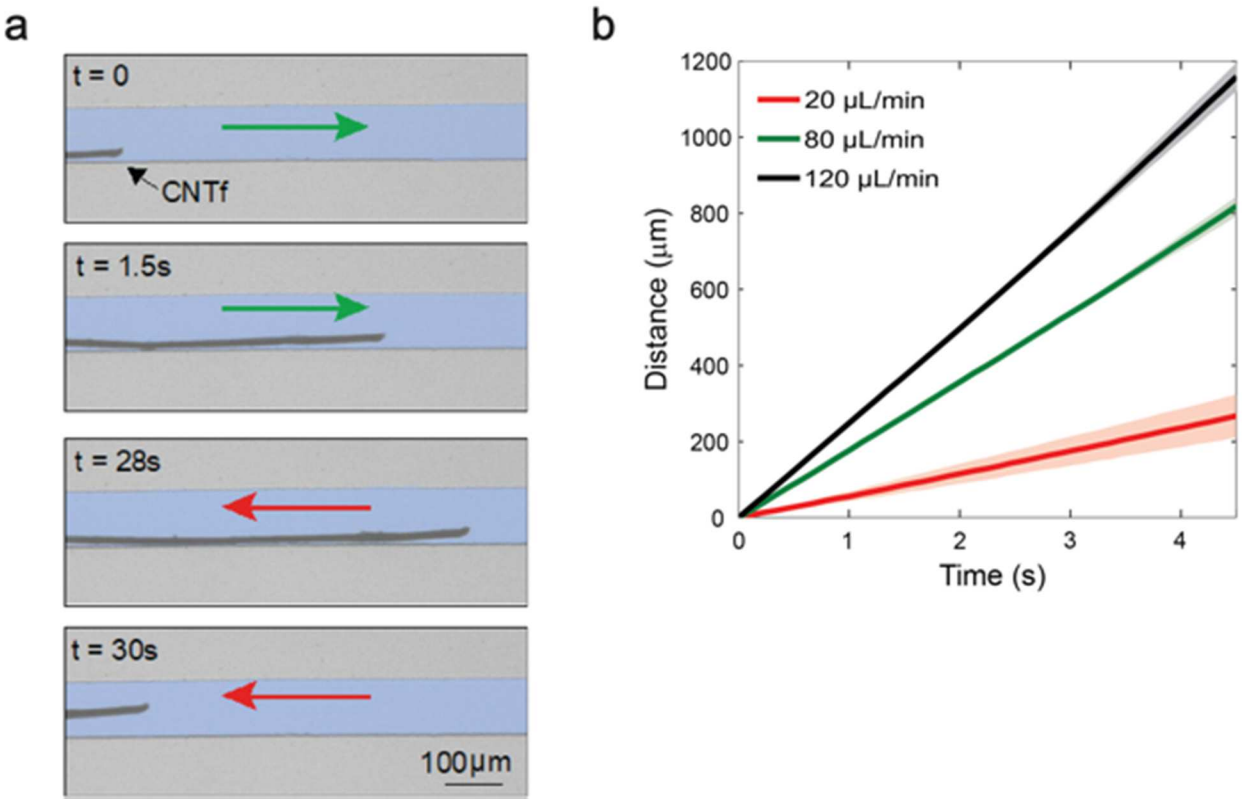

Figure S5. (a) Sequence of bidirectional actuation of CNTf inside the PDMS channel in response to the forward (top, green arrow) and reversed fluid motion (bottom, red panel). Input flow rate of 80 μL/min. (b) Distance traveled by the CNTf in the channel at varying forward flow rates. Lines indicate mean values and shaded areas represent standard deviation.

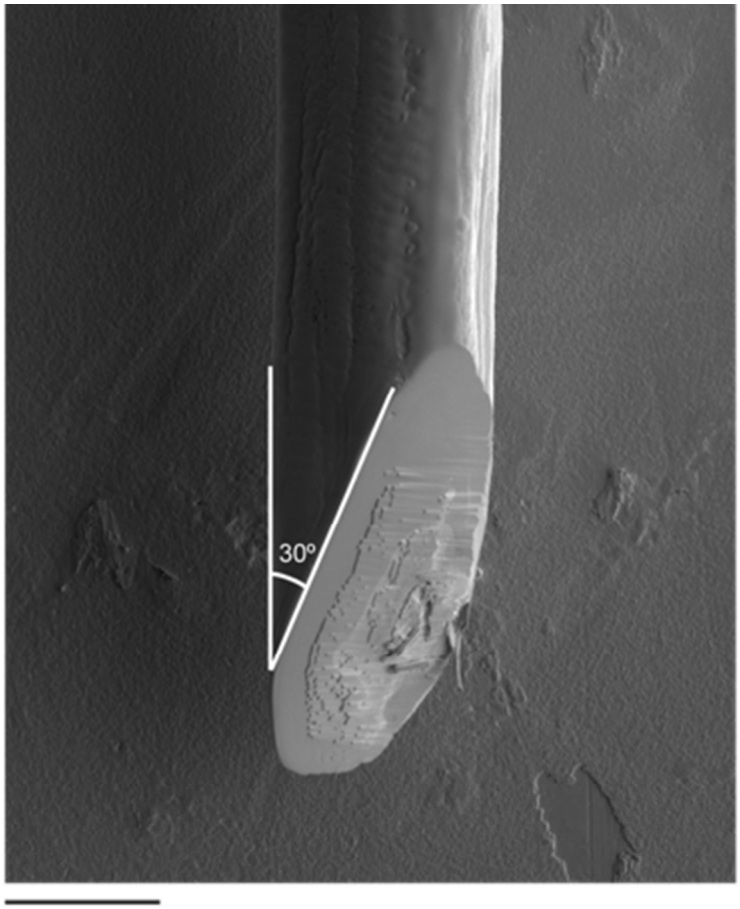

Figure S6. Parylene-coated CNTf sharpened to a 30 degree angle using Focused Ion Beam (FIB). Scale bar: 20 μm.

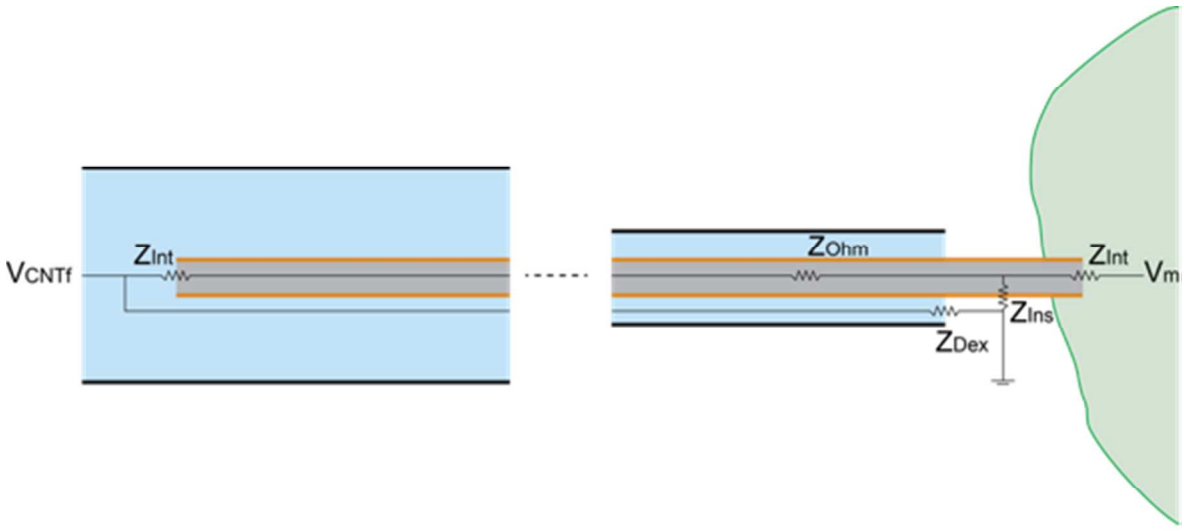

Figure S7. Equivalent circuit model of the fluidic actuated CNTf electrode. The right-most end of the CNTf (gray) is inserted into the tissue (green) while the left end remains in the microfluidic channel. The impedance of these two interfaces between the CNTf and the fluid is noted as Z_{int}. The CNTf is insulated along the length by a layer of oxide or Parylene-C as electrode (orange) with an insulator impedance of Z_{ins}. The conductive dextran solution (blue) creates an electrical contact at the left-most end of the fiber and enables us to actuate the fiber using fluid flow. This conductive solution also produces a short to ground which we mark as Z_{Dex}. The short to ground produces a voltage divider that reduces the magnitude of the CNTf recordings. Since Z_{Ins} is much larger than the Z_{Int} and the ohmic impedance of the fiber (Z_{ohm}) we can calculate the attenuation factor as $Z_{Dex}/(Z_{Dex}+2Z_{int})$. The overall device impedance converges to Z_{Dex} on the low frequency regime, which allows us to experimentally determine Z_{Dex} by analysing the frequency spectrum of the device impedance (Supplemental Figure S12). We estimate that $Z_{Dex} \approx 2Z_{int}$, which implies that the signal is attenuated by approximatelly 50%. Such attenuation, however, does not prevent us to record compound action potentials in *Hydra* and neuronal spikes in brain slices.

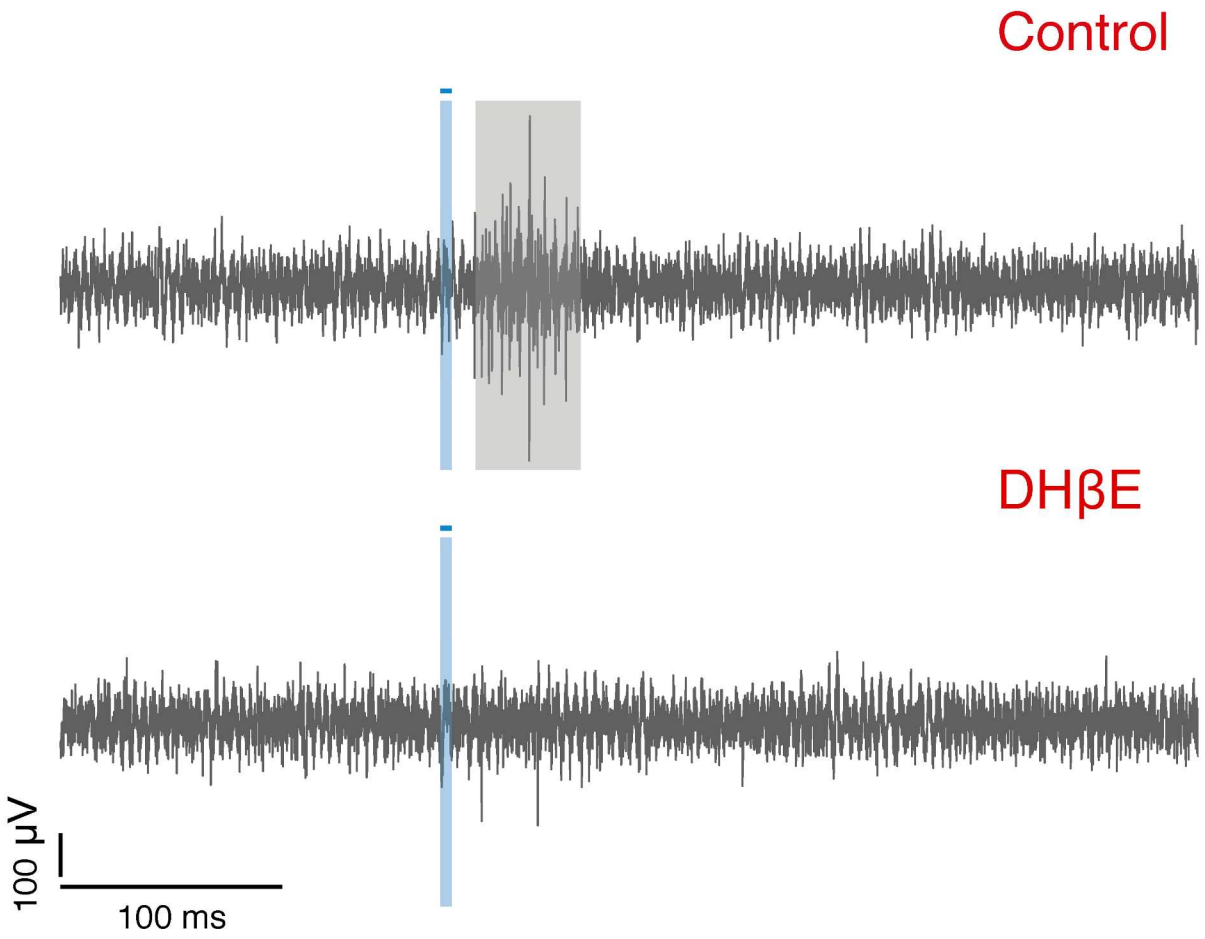

Figure S8. TRN neural activity recorded with microfluidic-actuated CNTf. TRN responses were evoked by light stimulation of ChR2-expressing cholinergic synaptic inputs and were blocked following bath-application of the nicotinic receptor antagonist DHβE (3 µM). The blue shaded area indicates timing of the 5 ms light pulse, and the grey shaded area indicates TRN neuronal activity.

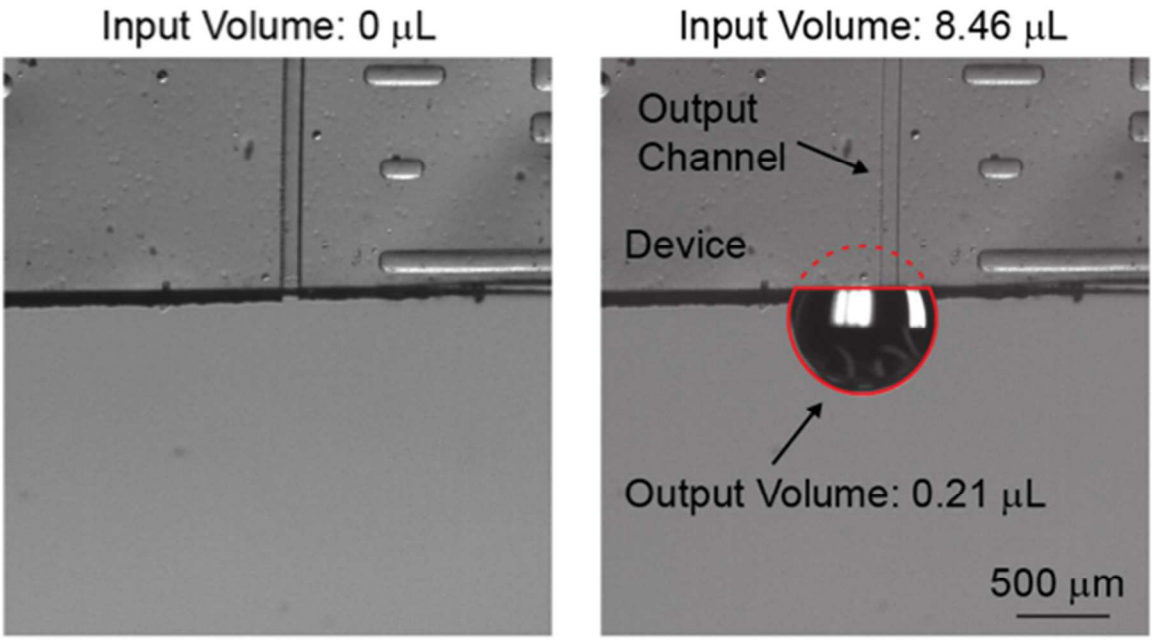

Figure S9. Volume of dextran ejected from the microdrive. The droplet formed at the output channel is modeled as a fraction of a sphere (red line). Based on this model we calculate the output volume to be 3.5±1.5% (n = 5 devices) of the input volume. To insert CNTfs 4 mm deep *in vivo*, we used an input volume of 14 ± 6 μL (n = 3 animals), which corresponds to an output volume of only 0.50 ± 0.23 μL.

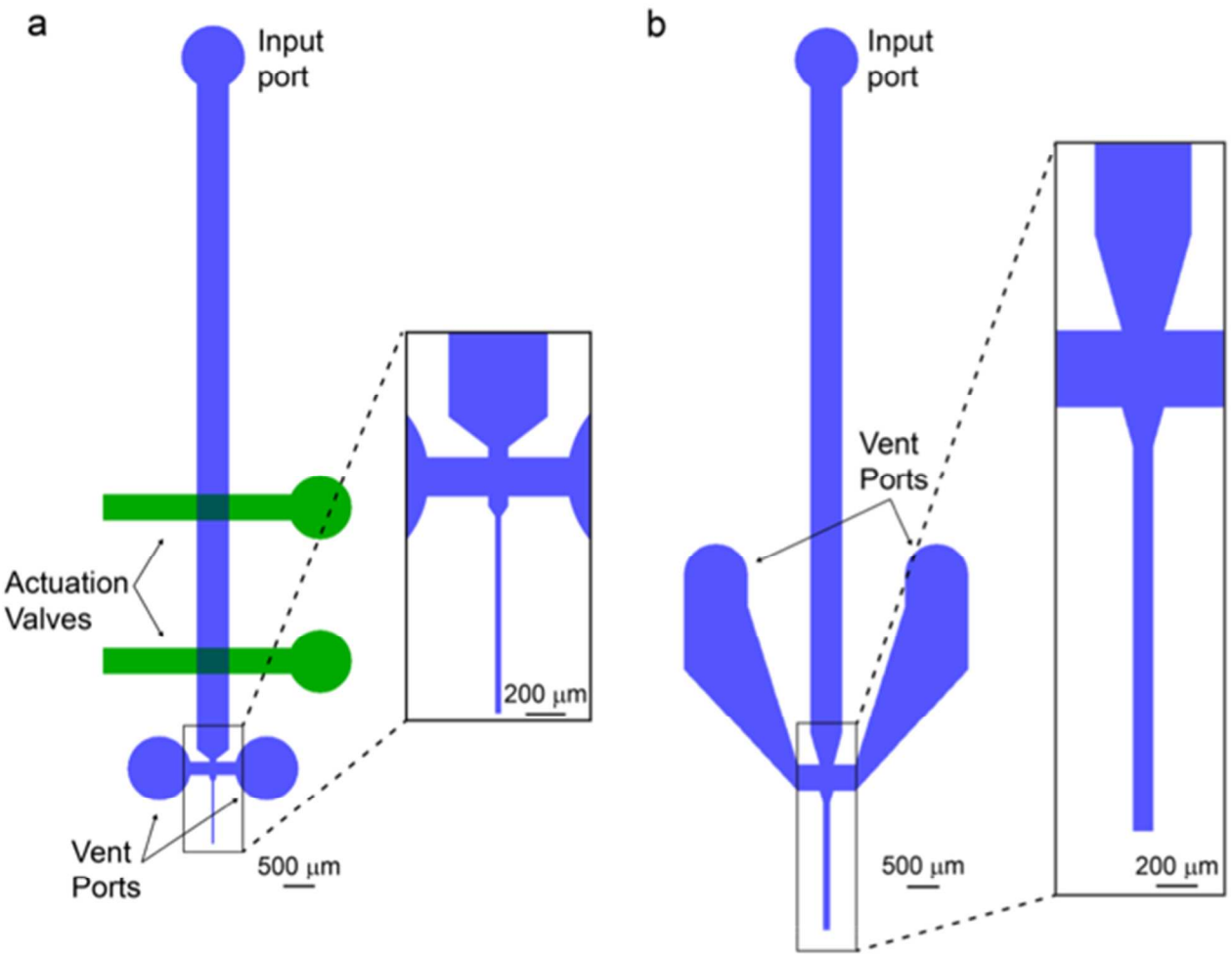

Figure S10. Microfluidic layouts for devices used for (a) *in vitro* (*Hydra* and brain slices) and (b) *in vivo* experiments. Channel height was 45 and 80 µm for the *in vitro* and *in vivo* devices respectively.

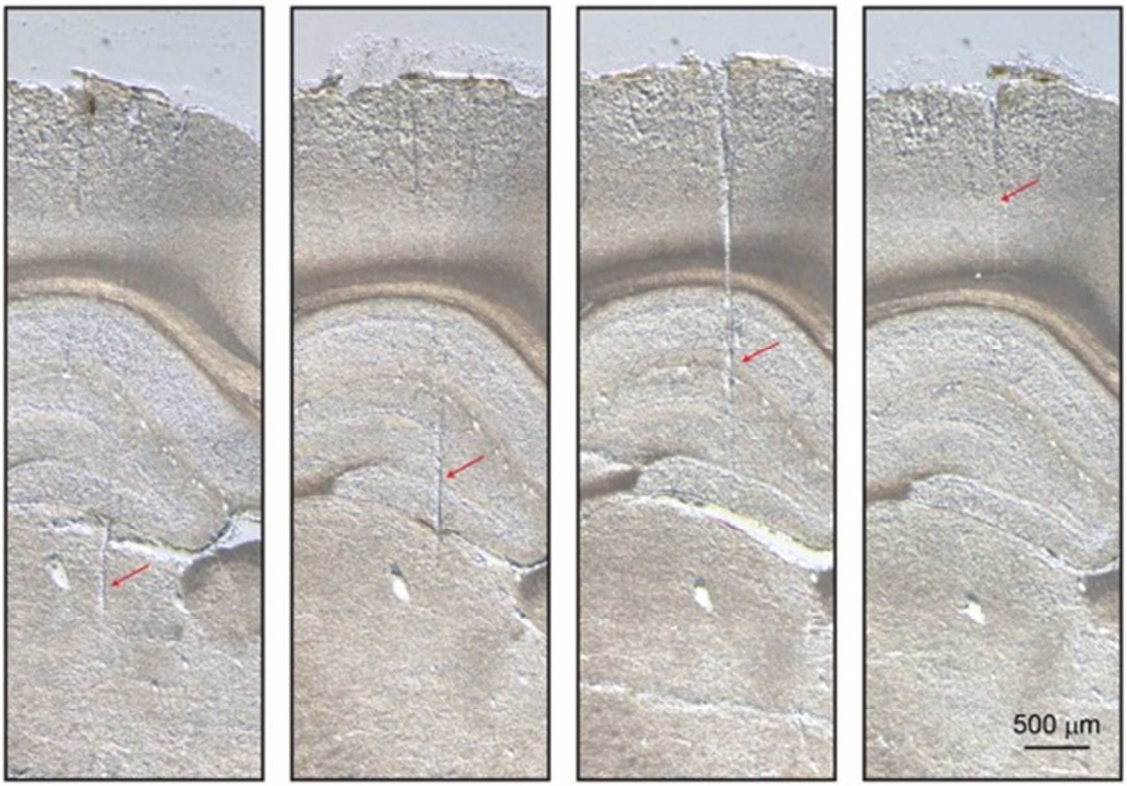

Figure S11. Coronal sections of a rat brain implanted with a 22 µm diameter CNTf using our microdrive. Each brain slice is 60 µm thick. Red arrows point to the microelectrode track, which crosses the hippocampus and ends in the thalamus.

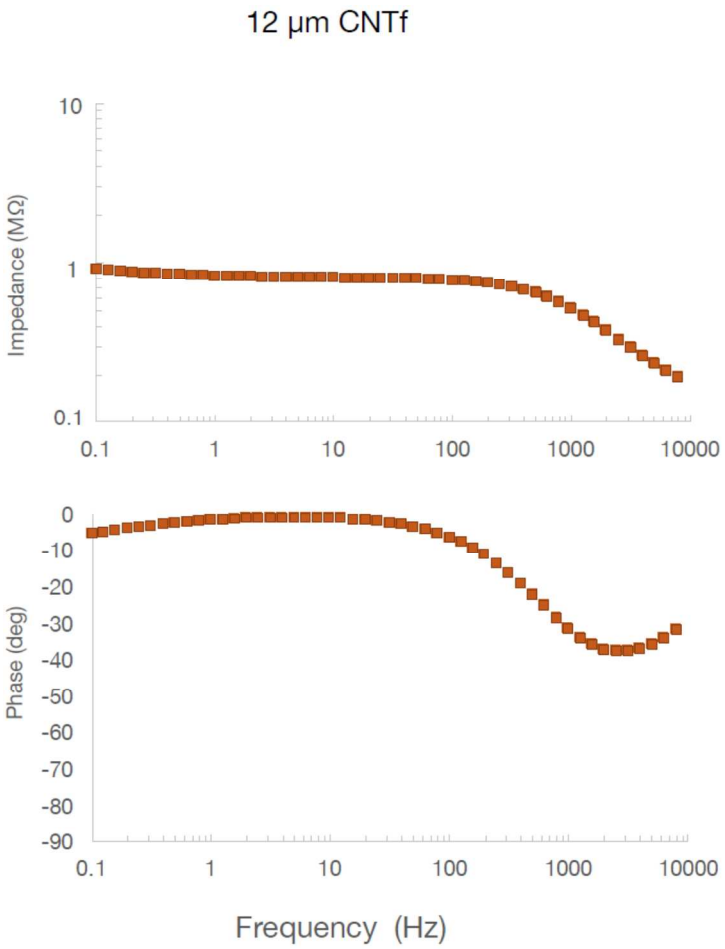

Figure S12. Representative impedance spectrum of our microdrive loaded with a 12 µm diameter microelectrode.

Materials and methods

Fabrication of CNTf microelectrodes. CNT fibers were fabricated from Meijo EC1.5-P CNTs (Meijo Nano Carbon Co., Ltd.) using a wet-spinning process previously reported.[7] Recordings from *Hydra* were obtained using CNTf coated with a dielectric double layer of Al_2O_3 and HfO_2 by Atomic Layer Deposition (ALD). To obtain a conformal coating, 12 µm diameter CNTfs were suspended between two glass slides separated by a few millimeters to prevent most of the fiber length from being in contact with a substrate. First, the fibers were exposed to an oxygen plasma cleaning process for a few minutes to clean residues and facilitate dielectric nucleation. Next, a standard ALD deposition (Cambridge Ultratech Savvanah S200) was performed. Al_2O_3 layer (50 nm) was grown using the precursors trimethylaluminum (TMA) and water and HfO_2 layer (25 nm) used tetrakis[dimethylamido]hafnium (TDMAH) and water. The process chamber was at 150°C and 1 Torr pressure with N_2 flowing at 20 sccm as carrier gas. Recordings from slices *ex vivo* and rat brain *in vivo* were obtained using Parylene coated fibers. Parylene C coating was preformed following standard protocols on a SCS Labcoter® 2 Parylene Deposition System. A donut shape acrylic holder was specially designed to load the fiber in the coating chamber allowing most of their length to be suspended. Scanning electron microscope (SEM) inspection indicates conformal and crack-free coating (Supplementary Figure S1).

Bending stiffness measurements. Bending modulus of insulated CNTf microelectrodes was measured using cantilever experiments,[8] using a similar setup to what described by Clapp et al.[9] CNTf samples of approximately 25 cm in length were hung vertically with a mass ~ 1.3 g in an oven at 115 °C for at least 4 hours. The fibers were then allowed to cool under tension for 6 hours in a glove box. This annealing process under tension was used to straighten the fibers and eliminate any bending history in them. Later, fibers were coated with parylene while still under tension. The straight insulated fibers were placed on a Teflon block and both ends were cut using sharp razor blade. One end of the fiber was clamped and opposite end was allowed to hang under self-weight as a cantilever in a glove box to minimize errors from air current disturbances. The fibers were slowly pulled backwards decreasing the cantilever length

until no deformation was observed. Photos of the cantilever were taken at different lengths using a Nikon Coolpix 900 digital single-lens reflex camera mounted on a tripod. The cantilever profiles were then mathematically processed using Matlab software and bending stiffness was calculated from fitting the measured deformation according to the *elastica* model, accounting for geometric non-linearities. Results of bending stiffness measurements on CNTf microelectrodes and comparison with other neural probes are reported in Supplementary Figure S3. Remarkably, due to relative shear sliding of the CNTs forming the fiber, the bending stiffness of CNTfs is not directly associated with the moment of inertia of the cross sectional area, even if it is here referred to as *EI* following the classical notation.[8]

Leakage current tests. The insulation coating thickness was measured with an ellipsometer (Filmetrics). The coating morphology was observed using both optical and electron microscopy to check for any defects. Furthermore, integrity of insulation coatings was assessed by measuring DC leakage currents and electrochemical impedance spectroscopy (EIS). Leakage currents were measured between insulated CNTfs (1 cm length) and a large carbon wire serving as counter and reference electrode at room temperature[10] on 1 cm of CNT fiber in PBS. A Gamry Reference 600 potentiostat (Gamry Instruments, input impedance 100 TΩ) was used to apply DC voltage bias of 1 V and the leakage current between the insulated CNT fibers and the counter electrode was measured. EIS measurements were performed with 20 mVpp input voltage in the range 1 Hz-100kHz between coated CNTf and the carbon counter electrode. Ag/AgCl electrode served as reference. To evaluate the mechanical stability of the coatings, we also measured leakage currents after the CNTf samples were bent at 5 different points, spaced 1 to 2 mm apart. CNTf were bent at 90^{o} by pressing them hard at a point and bending it across the point using tweezers. The bent fibers were immersed back in PBS and the leakage current measurement protocol was repeated. Negligible difference in the leakage current values before and after the bending of insulated CNT fibers suggest the mechanical stability of parylene coatings.

FIB patterning CNTf microelectrodes. To facilitate insertion and reduce damage in tissue, parylene coated CNTf with 22 and 25 μm in diameter were sharpened using

standard FIB (FEI Helios NanoLab 660 DualBeam) protocols. A 30kV gallium beam (65nA) was focused on the surface of the fiber to cut it at a 30° angle with respect to its axis.

Dextran rheology. Dextran viscosity measurements were carried out at room temperature with Advanced Rheometric Expansion System (ARES, Rheometrics Scientific, now TA Instrument) in a Couette geometry. A solution of 40 % w/w Dextran in DI was loaded in a titanium cup (diameter = 16.5 mm), which rotates relative to a titanium bob in the center of the cup. Viscosity was measured as a function of shear rate (test duration: 20 min, shear rate: 0.1 to 100 s^{-1}).

Microfluidic device fabrication. Double layer PDMS microfluidic devices were fabricated following standard soft-lithography technique. Briefly, Si wafers (University Wafer) were spin coated with SU-8 2050 (Microchem), followed by a photolithography process which defined valve and flow channels on two separate wafers. Next, a thin layer (approximately 70 μm) of flexible (20:1 Elastomer:Cross-linker, w/w ratio) PDMS (RTV615, Fischer Scientific Company LLC) was spin-coated on the flow channel patterned wafer. At the same time, a thick (approximately 2 mm, 5:1 Elastomer:Cross-linker, w/w ratio) PDMS was poured on the valve layer patterned wafer. Both wafers were baked in an oven at 90° C: 15 min for the flow layer and 45 min for the valve layer. After alignment of the flow and valve control layers, the devices were baked for additional 24 hours at 90°C.

CNTf microelectrodes with diameters of 12 μm (agarose, *Hydra*, and *in vivo* experiments), 22 μm (*in vivo* experiments) and 25 μm (CNTf actuation and slices experiments) and length between 7 and 10 mm were manually loaded in the PDMS device using carbon-tip tweezers. To seal the microfluidic device with the fiber, an oxygen plasma cleaning step (Harrick plasma PDC-001) on the PDMS and glass was performed, allowing for a strong and leak free covalent bound between their exposed surfaces. Each microelectrode was used only once per trial and never reused.

We found that overall device yield was approximately 80% with the most common failure mode being PDMS delamination. Plasma binding between PDMS and glass is extensively used in microfluidic devices operated under low pressures; however, the

high input pressure necessary to produce the high flow rates that drive microelectrodes in tissue can cause PDMS delamination. This delamination can produce undesirable leaks that reduce the velocity of the fluid flow. We expect that the inconsistency in the plasma binding may be due to the cleanliness of the PDMS surfaces or variability in the plasma density and gas ratios, and that improving these elements may increase device yield.

Measurement of ejected dextran volume. The volume of fluid ejected from the device through the exit channel was obtained by measuring the size of the dextran droplet formed at the output channel in the device geometry used for *in vivo* experiments. With no microelectrodes in the channel, we flowed 4.1 ± 2.5 µL (n = 5 devices) of dextran solution through the device and observed a droplet form at the output channel. By modeling this droplet as a fraction of a sphere (see Supplementary Figure S9) we estimated the volume fluid to be 3.5 ± 1.5% (n = 5 devices) of the input volume, which is lower than the theoretical value of 7% estimated from CFD simulations. This difference is likely due to variations on the channel geometry during device fabrication relative to the ideal computational model.

Brain phantom insertion tests. Agarose gel was used as brain phantom for insertion tests (Fig. 1 d and e). The gel was prepared by first mixing agarose (Sigma-Aldrich Corporation) with DI water on a 0.6% w/w concentration.[11] The solution was then heated in a microwave until boiling and finally left at room temperature to gelate at least 2 hours. For imaging purpose, a drop of red food colorant was added to the solution.
Microfluidics devices were loaded with parylene-coated 12 µm diameter CNTf microelectrodes as described above. The glass slide was vertically mounted on a micromanipulator and gently brought in contact with the agarose gel. To insert the fiber in agarose, manual pressure was applied to the syringe filled with a blue Dextran solution (40% w/w in DI with blue food colorant) connected to the fiber input port (Supplementary Video M1).
Manual CNTf insertion attempted by moving a similar fiber vertically towards the agarose gel using a self-closing tweezer assembled on a micromanipulator. The CNTf was held approximately 4 mm away from the edge and the micromanipulator was

manually operated to move the fiber at an average speed of approximately 0.3 mm/s (Supplementary Video M2).

Tissue phantom actuation test. Microfluidic devices loaded with FIB-sharpened, 25 μm diameter CNT fibers were fabricated as described above and horizontally attached in a petri dish. Valve channels were filled with DI water and connected to a valve controller. A Matlab (Mathworks Inc.) script was used to switch between Closed and Open valve states. A cubic block of agar gel (0.6 % w/w in DI prepared as described above) approximately 1 cm^3 was gently placed in contact with the exit channel of the device. To drive the fiber, manual pressure was applied to the syringe filled with Dextran solution (40% w/w in DI) connected to the fiber input port. A video of the fiber movement in agar was collected at approximately 8.9 fps using Hamamatsu Orca 03-G camera mounted on an inverted Nikon scope. A Matlab script was used to isolate the fiber from the background and determine the position of the distal end.

Device impedance in Hydra and brain slice experiments. To measure impedance of the devices used in *Hydra* and brain slices experiments, the CNTf microelectrode was inserted in the fluidic microdrive and connected on one end to the working Ag/AgCl electrode through the conductive Dextran solution, which is made by mixing Dextran with PBS. The distal end of the microelectrode was advanced inside a 1x PBS bath. A Ag/AgCl immersed in the PBS bath was used as a reference and counter electrode. Although the distance between the back of the CNTf electrodes and the Ag/AgCl electrode changes as the electrode drives into tissue, we expect the impedance of this liquid junction to only change by approximately 15 kΩ, as determined by $\mathrm{Z} = \rho\Delta\mathrm{L}/(\mathrm{w} \cdot \mathrm{d})$, where ρ is the solution resistivity (0.259 ± 0.006 kΩ·mm, n = 3 devices), ΔL is the electrode distance variation (1.5 mm), w is the channel width (0.5 mm), and h is the height (50 μm). Moreover, we can minimize this effect base on the placement of the Ag/AgCl electrode. For example, for a 4 mm deep insertion, the distance between the CNTf and the Ag/AgCl electrode changes by only 1.5 mm by placing the Ag/AgCl port (1 mm in diameter) 1.5 mm upstream of the fiber back end. Based on a change in impedance of only ∼15 kΩ we do not expect the overall signal quality to be affected. Increasing the ionic concentration of the driving solution can further reduce the liquid

junction impedance at the risk of also reducing the stray impedance to ground.

***Hydra* culture.** *Hydra* (*H. littoralis* obtained from Carolina Biological Supply Company) were cultivated in plastic vials at room temperature in standard *Hydra* culture medium (protocol adapted from Steele lab). The animals were fed once every two days with freshly hatched brine shrimps (*Artemia naupli)*. Before electrophysiology experiments *Hydras* were food deprived for 24 hours.

***Hydra* electrophysiology.** A glass slide containing both the fluidic microdrive and the *Hydra* trap was fixed to a plastic Petri dish filled with *Hydra* media. *Hydra* (n=3) with length between 1.5 and 2.0 mm were randomly selected and partially immobilized by the *Hydra* trap. This was accomplished by positioning the animal using a glass pipette next to the trap channels, followed by application of negative pressure at the trap port. Next, 12 μm in diameter CNTf microelectrodes (138 ± 33 kΩ, microelectrode impedance, n = 3 CNTfs, final device impedance 663 ± 127 kΩ, n = 3 devices, 10 mV, 1 kHz) were actuated towards the *Hydra* by applying manual pressure to a syringe connected to the fiber input port and filled with a conductive dextran solution (40% w/w in 1x PBS). Valves were actuated (opened and closed) to guarantee precise positioning of the fiber inside or next to the animal.
The working Ag/AgCl electrode was placed in contact with the conductive Dextran solution in the microfluidic channel while the reference Ag/AgCl electrode was placed in the *Hydra* medium. Data were collected by using an AM Systems model 1800 amplifier (input impedance 100 MΩ) and a Digidata 1550 digitizer (Molecular Devices) at 10 kHz sampling rate with 0.5 Hz low-cut filter and 20 kHz high-cut filter.

Fluid dynamic analysis. Flow simulations were performed using Comsol (Comsol Inc.). Stationary Navier-Stokes equation was solved in laminar flow regime using a finite element method applied to a 3D model of the device layout. Boundary conditions were set to constant pressure of 10 atm at the inlet port and 1 atm at the outlet port and no-slip on the sidewalls.

Buckling analysis. Critical buckling load of microelectrodes was obtained by solving an eigenvalue-based linear buckling analysis under stationary conditions using Comsol

(Comsol Inc.). CNTfs were modelled as Euler-Bernoulli beams with 1 mm in length and 12 μm in diameter. A fixed constraint was set to one of the extremes and a unitary load directed towards this fixed boundary was applied. This load was either concentrated on the free extreme or distributed along the CNTf length. These calculations show that the critical buckling load for the distributed load scenario is approximately 3 times higher than the concentrated load case.

Brain slice preparation. Young mice (male and female) were randomly selected from two lines (P13-21): C57BL/6J wild-type (n = 3 animals) and bacterial artificial chromosome (BAC)-transgenic mice (n = 3 animals) expressing channelrhodopsin-2 (ChR2) under the control of the choline acetyltransferase (ChAT) promoter (ChAT–ChR2–EYFP). Wild-type and transgenic animals were used for recordings in cortex (Figure 4B and C) and in TRN (Figure 4e and f), respectively. Thalamocortical slices (400 μm) were prepared as described previously.[12] Animals were anesthesized with isofluorane and decapitated, following procedures in accordance with NIH guidelines and approved by the UTHealth animal welfare committee. Slices (450 μm) were cut in an ice-cold solution consisting of (in mM): 234 sucrose, 2.5 KCl, 1.25 NaH2PO4, 10 MgSO4, 26 NaHCO3, 10 glucose, and 0.5 CaCl2, saturated with 95% O2-5% CO2, using a vibratome (Leica VT1200S) at speeds of 0.2 mm/s and a blade vibration amplitude of 0.8 mm. Slices were incubated at 34°C for 40 min in artificial cerebrospinal fluid (ACSF) containing (in mM): 126 NaCl, 26 NaHCO3, 2.5 KCl, 1.25 NaH2PO4, 10 glucose, 2 CaCl2, and 2 MgCl2. Slices were then kept at room temperature prior to recordings.

Brain slice electrophysiology. Fluidic microdrives were sealed at the edge of a 500 μm thick glass slide and mounted on a 60 mm-diameter plastic petri dish. Tubes for ACSF perfusion were placed on opposing sides of the dish. Freshly dissected 450 μm brain slices were placed on a 150 μm thick glass slide pre-coated with poly-L-lysine (Sigma Aldrich). The brain slice was manually positioned as close as possible to the device with cortex facing the fiber exit channel. All recordings were carried out at near-physiological temperatures (32-34 °C).

CNTf microelectrodes (25 μm diameter, 355 ± 93 kΩ microelectrode impedance, n = 3

CNTfs, final device impedance 261 ± 16 kΩ, n = 2 devices, 10 mV, 1 kHz) were inserted into brain slices by applying manual pressure to a syringe connected to the fiber input port and filled with a highly conductive Dextran solution (40% w/w in 20x PBS). Valves were actuated (opened for 100ms and closed for 900ms) to guarantee precise positioning and actuation of the fiber inside the brain slice. For cortical recordings, the microelectrode was actuated until spikes were visible in the electrical recording (n = 3 slices, each from different animals).

The working Ag/AgCl electrode was placed in contact with the conductive Dextran solution in the fiber channel while the reference Ag/AgCl electrode was placed in contact with the ACSF bath in the dish. Data were collected by using an AM Systems model 1800 amplifier and a Digidata 1550 digitizer (Molecular Devices) at a 50 kHz sampling rate with 0.5 Hz lowpass filter and 20 kHz highpass filter.

In all experiments on brain slices extracted from transgenic mice, when the microelectrode tip was in the TRN we recorded light-evoked activity (n = 3 animals). For microelectrodes with thin parylene insulation layers (1.2 μm), we also observed light-evoked activity after we actuated the tip through the TRN leaving the insulated portion within the TRN (n = 2 animals). To prevent electrical recording through the insulating layer we increased the parylene coating thickness to 3.3 μm. Under this condition, we recorded activity exclusively from the tip (Figure 3e and f, n = 1 animal). Thickness of TRN was measured in n = 4 brain slices used for experiments. The mean thickness was calculated by averaging the values of 3 regions in a given slice. Optical stimulation was performed using a DL447 laser (Crystalaser) at a wavelength of 440–447 nm. Single laser pulses of 5 ms duration and 5 mW power were used to activate cholinergic afferents in the TRN.

Impedance to ground. To estimate the impedance to ground through the conductive Dextran solution (Z_{Dex}, Supplementary Figure S7) during Hydra and brain slice recordings, we analyzed the impedance spectrum of devices loaded with microelectrodes (Supplementary Figure S12). We expect the device impedance to converge to Z_{Dex} at very low frequencies. At frequencies below 10 Hz we found that the impedance stabilized near 1.5 MΩ which we expect to be primarily the DC impedance through the dextran solution. This impedance to ground was roughly twice the interfacial

impedance of the CNTf ($Z_{Dex} \approx 2Z_{int}$), which implies that the signal is attenuated by approximately 50%. Such attenuation, however, does not prevent us to record compound action potentials in *Hydra* and neuronal spikes in brain slices.

Neural recording *in vivo* in rats. Long-Evans rats (1 male and 2 females between 4 and 21 months old for 12 μm diameter microelectrode, and 1 male and 2 females between 3 and 22 months old for 22 μm diameter microelectrode, randomly selected) were used for our acute *in vivo* recordings. All the procedures were approved and monitored by the Rice University Institutional Animal Care and Use Committee. Rats were given buprenorphine (0.02 mg/kg) then induced under 5% isoflurane and maintained at 1-2.5% isoflurane for the duration of surgery and recording. After the initial incision and cleaning of the skull, two screws were placed in burr holes made over right frontal cortex (roughly 1.5 mm anterior and 2 mm lateral to bregma) and over the cerebellar bone for use as an EEG screw and ground screw, respectively. Next, a craniotomy was drilled over the left parietal lobe centered at 2 mm lateral and 3 mm posterior to bregma and dura over part of the exposed brain was removed. The fluidic microdrive was attached to a stereotaxic arm, centered and lowered over the durotomy. Once lowered, fluid pressure was applied to the input port via a tube connected to a syringe filled with dextran. Once pressure at the input port began to flow the dextran solution through the microchannel, the microelectrode proceeded to move and was implanted into the brain over the course of 5-10 seconds (Supplementary Video M4). In practice, the fluid injection parameters are adjusted during the experiment based on the fiber displacement. Once the fiber begins moving we can adjust the flow rate to achieve the desired velocity and penetration depth by monitoring the fiber displacement in the microfluidic device using a microscope or magnification optics. After the implantation was complete, the microdrive was slowly retracted with the stereotaxic arm while slight positive pressure was applied to prevent the probe from being retracted with the device (Supplementary Video M6). Once the CNTf microelectrode was free from the microdrive, another stereotaxic arm with a recording wire attached to it was brought close to the exposed end of the microelectrode. Ag paint (Silver Print II, GC Electronics) was applied to the recording wire and then the recording wire and microelectrode were brought together bridged by the Ag paint. After allowing the Ag paint to dry for 5

minutes, *in vivo* impedance spectroscopy was performed in the two-electrode configuration, using the fibers as working electrode and the skull screw as a reference. Impedance spectra were acquired by applying a 10 mV AC voltage in the 100 mHz to 1 kHZ range with a Gamry 600+ potentiostat. The average impedance of the CNTf microelectrode used *in vivo* was 430 ± 140 kΩ (22 μm in diameter, n = 3 CNTfs) and 138 ± 33 kΩ (12 μm in diameter, n=3). Note that the 22 μm diameter CNTf was sharpened using FIB to reduce tissue damage. This process increases the electrode impedance likely due to local heating, which can lead to the formation of amorphous carbon that can increase the interfacial impedance.

The recording wire was retracted in steps of 150 to 500 μm and recordings were taken at each step. During retraction, the electrode was visually monitored under magnification, and absolute implantation depth for each recording was inferred from the depth at which the electrode exited the brain.

Histological verification of *in vivo* implantation. One male Long Evans rat was implanted with a 22 μm diameter microelectrode using the fluidic microdrive as described above. Immediately after implant, the rat was transcardially perfused with isotonic sucrose followed by 4% paraformaldehyde (PFA) while under deep isoflurane anesthesia. The brain was then extracted from the skull without disturbing the microelectrode and left to post-fix in PFA for 24 hours, then cryoprotected in 30% sucrose until the brain sunk (about 48 hours). After cryoprotection, the brain was mounted on a cryostat (Leica Microsystems) and cut into coronal sections 60 μm thick until the microelectrode was visible.

Brain slice and *in vivo* data analysis. Electrophysiological recordings were analyzed and processed off-line with a custom Matlab (Mathworks Inc.) script. To isolate spikes, the raw data stream was first digitally filtered between 300 Hz and 6 KHz. Spike detection was performed on the bandpass filtered data based on an amplitude threshold automatically set as 4.5 times the estimated standard deviation of the noise.[13] Principal components of the waveforms were calculated on a 3 ms window isolated from the threshold-crossing spikes followed by unsupervised clustering and sorting.

References

(1) Shen, W.; Karumbaiah, L.; Liu, X.; Saxena, T.; Chen, S.; Patkar, R.; Bellamkonda, R. V.; Allen, M. G. *Microsyst. Nanoeng.* **2015**, *1*, 15010.

(2) Kozai, T. D. Y.; Langhals, N. B.; Patel, P. R.; Deng, X.; Zhang, H.; Smith, K. L.; Lahann, J.; Kotov, N. A.; Kipke, D. R. *Nat. Mater.* **2012**, *11* (12), 1065–1073.

(3) Rousche, P. J.; Normann, R. A. *IEEE Trans Rehabil Eng* **1999**, *7* (1), 56–68.

(4) Subbaroyan, J.; Martin, D. C.; Kipke, D. R. *J Neural Eng* **2005**, *2* (4), 103–113.

(5) Nicolelis, M. A. L.; Dimitrov, D.; Carmena, J. M.; Crist, R.; Lehew, G.; Kralik, J. D.; Wise, S. P. *Proc. Natl. Acad. Sci. U.S.A.* **2003**, *100* (19), 11041–11046.

(6) Chen, R.; Canales, A.; Anikeeva, P. *Nature Reviews Materials* **2017**, *1* (2), 1–16.

(7) Behabtu, N.; Young, C. C.; Tsentalovich, D. E.; Kleinerman, O.; Wang, X.; Ma, A. W. K.; Bengio, E. A.; Waarbeek, ter, R. F.; de Jong, J. J.; Hoogerwerf, R. E.; Fairchild, S. B.; Ferguson, J. B.; Maruyama, B.; Kono, J.; Talmon, Y.; Cohen, Y.; Otto, M. J.; Pasquali, M. *Science* **2013**, *339* (6116), 182–186.

(8) Adnan, M. Solution processing of boron nitride nanotubes and bending behavior of carbon nanotube fibers. *Ph.D. Thesis*, Rice University. **2016**.

(9) Clapp, T. G.; Peng, H.; Ghosh, T. K. *Textile Research …* **1990**, *60* (9), 525–533.

(10) Cogan, S. F.; Edell, D. J.; Guzelian, A. A.; Ping Liu, Y.; Edell, R. *J Biomed Mater Res A* **2003**, *67A* (3), 856–867.

(11) Chen, Z.-J.; Gillies, G. T.; Broaddus, W. C.; Prabhu, S. S.; Fillmore, H.; Mitchell, R. M.; Corwin, F. D.; Fatouros, P. P. *Journal of Neurosurgery* **2004**, *101* (2), 314–322.

(12) Agmon, A.; Connors, B. W. *Neuroscience* **1991**, *41* (2-3), 365–379.

(13) Quiroga, R. Q.; Nadasdy, Z.; Ben-Shaul, Y. *Neural Comput* **2004**, *16* (8), 1661–1687.